

$^{22}\text{Ne}(\alpha, n)^{25}\text{Mg}$: The Key Neutron Source in Massive Stars

M. Jaeger,¹ R. Kunz,¹ A. Mayer,¹ J. W. Hammer,¹ G. Staudt,² K. L. Kratz,³ and B. Pfeiffer³

¹*Institut für Strahlenphysik, Universität Stuttgart, D-70550 Stuttgart, Germany*

²*Physikalisches Institut, Universität Tübingen, D-72076 Tübingen, Germany*

³*Institut für Kernchemie, Universität Mainz, D-55128 Mainz, Germany*

(Received 15 February 2001; revised manuscript received 24 July 2001; published 24 October 2001)

The excitation function of the reaction $^{22}\text{Ne}(\alpha, n)^{25}\text{Mg}$, the key neutron source in the astrophysical s process in massive stars, has been determined from threshold at $E_\alpha = 570$ up to 1450 keV with an experimental sensitivity of 10^{-11} b. For all resonances in this energy range new resonance parameters have been measured. For a possible resonance at about 635 keV a new upper limit $\omega\gamma < 60$ neV for the strength was obtained. Based on the new data, improved reaction rates were calculated as a function of temperature. The new uncertainty limits are considerably smaller than in previous determinations, ruling out the large enhancement factors, up to 500, assumed in some stellar model calculations.

DOI: 10.1103/PhysRevLett.87.202501

PACS numbers: 25.55.-e, 24.30.-v, 26.20.+f, 27.30.+t

The reaction $^{22}\text{Ne}(\alpha, n)^{25}\text{Mg}$ is the dominant source of neutrons for the s process (neutron capture on a slow time scale) in massive stars with $M > 8M_\odot$ ($M_\odot =$ solar mass) destined to become supernovae [1]. Calculations suggest that this range of stellar masses is responsible for producing most of the nuclides attributed to slow neutron capture for atomic masses $A \sim 60$ –90 as well as many lighter than $A = 60$ [2]. The remainder of the s process ($A \sim 90$ –209) is thought to be produced in asymptotic giant branch (AGB) stars by a combination of the $^{13}\text{C}(\alpha, n)^{16}\text{O}$ and $^{22}\text{Ne}(\alpha, n)^{25}\text{Mg}$ reactions during the helium shell flashes that characterize these stars [3]. Helium accumulates in a layer overlying the inert degenerate carbon nucleus of the AGB star and ignites at intervals of typically 10^4 – 10^5 years.

The $^{22}\text{Ne}(\alpha, n)^{25}\text{Mg}$ reaction rate at energies appropriate for helium burning [$(2$ – $3) \times 10^8$ K] has been the subject of intensive investigation for years [4–10], resulting in data sets and evaluated reaction rates, which differ from one another considerably [8, 11–13], far beyond what is acceptable for stellar model calculations. For example, Costa *et al.* [14] investigated the influence of the $^{22}\text{Ne}(\alpha, n)^{25}\text{Mg}$ rate on the abundances of s -nuclide seeds for the p process [15], which is thought to take place in the O and Ne layers of type II supernovae. On the basis of the uncertainties quoted by the NACRE compilation [11], these authors [14] introduced enhancement factors in the range between 5 and 500 above the adopted rate. Only by using such greatly enhanced rates—at least with factors of 10 to 50—in a $25M_\odot$ stellar model could a severe underproduction of light Mo and Ru isotopes be cured. The *et al.* [16] studied the s process in stellar models with $M = (15$ – $30)M_\odot$ with an extended reaction network to obtain the s process yields for different assumed rates for the reactions $^{22}\text{Ne}(\alpha, n)^{25}\text{Mg}$ and $^{12}\text{C}(\alpha, \gamma)^{16}\text{O}$. These calculations also favor an enhanced $^{22}\text{Ne}(\alpha, n)^{25}\text{Mg}$ reaction rate at low temperatures to strengthen the s process. Clearly for stellar models involving the $^{22}\text{Ne}(\alpha, n)^{25}\text{Mg}$ reaction, its rate should be determined within much nar-

rower limits. However, $^{22}\text{Ne}(\alpha, n)^{25}\text{Mg}$ competes with the $^{22}\text{Ne}(\alpha, \gamma)^{26}\text{Mg}$ reaction and therefore the absolute cross sections of both of these reactions are needed.

The experiment was performed at the Stuttgart DYNAMITRON accelerator with a He^+ beam of about 1 mm diameter at the windowless gas target facility RHINOCEROS. The 99.9% enriched ^{22}Ne target gas was continuously recirculated to allow long term experiments in a specially designed reaction chamber with highly polished gold-plated walls. The high chemical purity of the gas was sustained by three purification elements: a cryogenic trap at liquid nitrogen temperature, a zeolite trap, and a getter purifier. The pressure was reduced by the differential pumping stages of the RHINOCEROS facility to several times 10^{-8} mbar. Some details of the experimental setup are presented in [17].

A new 4π neutron detector has been designed and tailored to this specific reaction. The reaction neutrons were thermalized in a cylindrical polyethylene moderator and subsequently captured by a setup of 12 proportional counters. The counters were arranged in two rings at radii optimized for the neutron energy of interest for this specific reaction. With this design, an absolute detection efficiency up to 50%, a low sensitivity for background neutrons, as well as some neutron energy information could be obtained simultaneously. The neutron detector assembly was surrounded by a plastic scintillator detector which served as a veto counter to suppress cosmic-ray-induced background. Several layers of passive shielding material (paraffin wax, polyethylene, boron, and cadmium) were arranged around the 4π neutron detector. Extensive simulations of the counter, the veto counter, and their geometry were performed. The calculations agreed within 5% with the experimental efficiency determinations. The background rate was determined by separate runs using the (α, n) -inactive isotopically enriched gas ^{20}Ne (99.9%), which has the same α -particle stopping power and straggling as ^{22}Ne . The excitation function of the $^{22}\text{Ne}(\alpha, n)^{25}\text{Mg}$ reaction was measured from threshold at

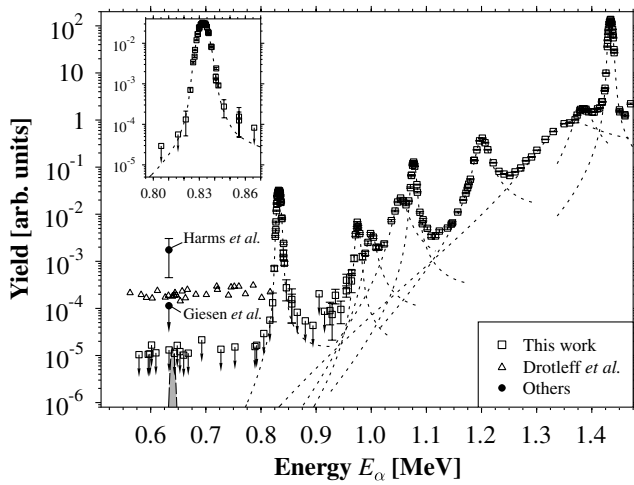


FIG. 1. Excitation function of $^{22}\text{Ne}(\alpha, n)^{25}\text{Mg}$ measured with the new experimental setup. The resonance at $E_\alpha = 832$ keV is shown in the inset. For comparison some data of previous measurements [6,8,9] have been plotted. The dashed curves show the fitted resonance functions. At the tails of the resonances the “yield” can be taken as cross section in (μb). The assumed resonance at 635 keV is shown as the shaded area with an upper limit for its strength of $\omega\gamma < 60$ neV.

$E_\alpha = 570$ keV up to 1500 keV with He^+ beam currents of 100–150 μA .

The parameters of the resonances in the measured energy range were derived from the excitation function. The final excitation function is given in Fig. 1 with the resonance at 832 keV shown in the inset. The calculated yield functions are shown as dashed curves. The results obtained for the resonance parameters are listed in Table I in comparison with the previous determinations of Drotleff *et al.* [8], and the compilations of Käppeler *et al.* [12] and Endt [18]. There are considerable differences between the

data sets; in particular, we have found that the positions, widths, and strengths of the resonances differ strongly from the data compiled recently by Endt [18]. For example, Endt quoted a width of less than 3 keV for all resonances of this reaction. Compared to Drotleff *et al.* [8], the $\omega\gamma$ value of the 832 keV resonance obtained here is smaller by about 34% which resulted from the much better spatial resolution of the new detector with its “short” ^3He counters. A previously unreported broad resonance was found at 1053 keV. Because of the improved resolution the resonance at 987 keV previously reported by Drotleff *et al.* [8] was resolved into two resonances with peaks at 976 and 1000 keV. We note that the strength used by Käppeler *et al.* [12] for the 832 keV resonance was the weighted average of the values obtained by Drotleff *et al.* [8] and Giesen *et al.* [9]. In the determination by Giesen *et al.* [9], where ^{22}Ne was implanted into a solid backing (“drive-in-target”), the neutron “signal” of the 832 keV resonance was less than 30% of the background yield; however, in the present work it is 2 orders of magnitude above background (see inset of Fig. 1), reflecting the huge improvement in the experimental sensitivity.

Our 4π neutron detector yields both the total counting rate as well as rough energy information derived from the ratio of counts in the inner and outer detector rings, the ratio being highly sensitive at neutron energies below 300 keV. Between threshold and 800 keV we measured in long runs a background yield which was the same for ^{20}Ne and ^{22}Ne and with and without α beam, which means explicitly that the entire measured yield between threshold and 800 keV is cosmic-ray-induced background. The “ratio” indicated clearly that the neutrons did not originate from the $^{22}\text{Ne}(\alpha, n)^{25}\text{Mg}$ reaction because of their high energy. Instead of subtracting background yields, the process

TABLE I. Resonance parameters (resonance energy E_{res} and width Γ in the laboratory system, resonance strength $\omega\gamma^a$ in the center-of-mass frame) for the reaction $^{22}\text{Ne}(\alpha, n)^{25}\text{Mg}$ at low energies (with uncertainties in brackets). The values for the resonance strength of the hypothetical resonance at about 635 keV are upper limits; its energy value was taken from [9,19,20].

This work				Drotleff (1993) [8]			Käppeler (1994) [12]	Endt (1998) [18]		
E_{res} (keV)	E_x (keV)	Γ (keV)	$\omega\gamma$ (meV)	E_{res} (keV)	Γ (keV)	$\omega\gamma$ (meV)	$\omega\gamma$ (meV)	E_{res} (keV)	Γ (keV)	$\omega\gamma$ (meV)
635(10)	11 152(10)	...	<60 neV	<520 neV ^b	623(6)
832(2)	11 319(2)	0.25(17)	0.118(11)	831(3)	<3	0.180(30)	0.200(36)	830(3)	<3	0.08(2)
976(2)	11 441(2)	2.1(9)	0.034(4)
...	987(10)	30(15)	0.16(10)	...	988(5)	<3	0.25(7)
1000(2)	11 461(2)	9.3(25)	0.048(10)
1053(2)	11 506(2)	12.7(25)	0.35(6)
1077(2)	11 526(2)	1.8(9)	0.83(7)	1076(10)	9(5)	1.9(5)	...	1066(5)	<3	1.6(4)
...	1178(5)	<3	4.9(1.2)
1200(2)	11 630(2)	13.5(17)	8.5(10)	1202(4)	19(3)	10.6(1.5)	...	1219(5)	<3	4.8(1.2)
1340(10)	11 749(10)	63.5(85)	60(9)	1350(10)	65(20)	55(20)
1385(4)	11 787(4)	24.5(34)	50(7)	1384(5)	25(10)	23(15)	...	1395(10)	<3	15(4)
1434(2)	11 828(2)	1.10(25)	1067(42)	1434(3)	<3	1105(120)	...	1433(2)	<3	610(90)

^a $\omega\gamma = \{(2J_r + 1)/[(2J_1 + 1)(2J_2 + 1)]\}[\Gamma_\alpha\Gamma_n/\Gamma]$, where $J_1 = J_2 = 0$, and J_r is assumed to be 1, except for the resonances at 832 and 1434 keV with $J_r = 2$. Γ_α , Γ_n , and Γ are the α width, the neutron width, and the total level width, respectively.

^bIn [9] this value was 740 neV.

TABLE II. Reaction rate $N_A \langle \sigma v \rangle$ of $^{22}\text{Ne}(\alpha, n)^{25}\text{Mg}$ in the temperature range $0.1 \leq T_9 \leq 1$ compared with three compilations: NACRE [11], Käppeler *et al.* [12], Caughlan and Fowler (CF88) [13]. The power of 10 for each line is given in the second column; temperature in units of $T_9 = T/(10^9 \text{ K})$, reaction rate in units of $\text{cm}^3 (\text{mols})^{-1}$.

T_9	Expt.	This work			NACRE			Käppeler <i>et al.</i>			CF88 Adopt.
		Recomm.	High	Low	Adopt.	High	Low	Tentative	High	Low	
0.10	-30	1.94	18	0.16	221	442	0.001	87
0.12	-26	5.07	49	0.21	23.3	12 000	1.0	524	1050	0.035	95
0.14	-23	7.34	70	0.42	19.6	14 400	1.1	675	1350	0.45	99
0.16	-20	1.89	16	0.33	3.5	3200	0.5	142	283	0.53	26
0.18	-18	1.79	11	0.75	2.7	2220	0.9	90	178	1.25	18.7
0.20	-16	0.88	3.5	0.59	1.2	670	0.7	25	49	0.98	5.3
0.25	-13	1.60	2.6	1.48	2.3	314	1.8	11.4	21	2.40	2.4
0.30	-11	2.69	3.2	2.63	4.1	192	3.4	9.1	14.4	4.14	1.9
0.35	-9	1.05	1.1	1.04	1.7	37	1.4	2.6	3.7	1.60	0.56
0.40	-8	1.63	1.70	1.63	2.6	34	2.2	3.5	4.7	2.43	0.91
0.50	-6	0.86	0.88	0.86	1.3	8.3	1.1	1.53	1.92	1.15	0.71
0.60	-5	1.92	1.97	1.88	2.5	8.0	2.1	2.57	3.21	1.93	1.9
0.80	-3	2.85	3.04	2.65	2.7	3.6	2.4	2.59	3.34	1.89	2.3
1.00	-2	8.73	9.59	7.86	7.8	8.9	7.0	7.11	9.25	5.27	6.6

that we used for $E_\alpha > 850 \text{ keV}$, we calculated (within 2σ) a worst case fraction for the reaction neutrons of 50–70 keV which is just consistent with the ratio and the yield. In this way we obtained a conservative upper limit for the yields in that neutron energy range, and an upper limit of $\omega\gamma < 60 \text{ neV}$ for the resonance strength of the possible resonance at about 635 keV, a factor of 9 smaller than the value of Giesen *et al.* [9,12], deduced from the α -transfer reaction, $^{22}\text{Ne}(^6\text{Li}, d)^{26}\text{Mg}$. We adopted the arguments of [9] that at most one state in ^{26}Mg , among the possible states identified by (γ, n) [19] or (n, γ) [20] experiments, has natural parity, and is thus a candidate for a resonance at about 635 keV.

New reaction rates were obtained by calculating the folding integral between the excitation function and the stellar Maxwell-Boltzmann distribution (see Table II). To arrive at the “recommended” rate we incorporated all resonances from Table I except one: the strength of the hypothetical resonance at 635 keV was taken to be 10% of its upper limit (6 neV) because its existence is still uncertain; here we have chosen the same fraction as in [12]. For the total width we took the value 24.6 eV given by [20].

For this calculation it was important to use not only the strengths but also the widths of the resonances. As can be seen in Fig. 1, the low energy tails of the broad resonances extend into the energy range below $E_\alpha = 800 \text{ keV}$. The measured excitation function could be well described by the resonances of Table I without the assumption of a background level or a constant S factor below 830 keV. Above $E_\alpha = 1450 \text{ keV}$ we used the data of Drotleff *et al.* [8] and above 2300 keV the data of Haas and Bair [4]. For the calculation of the “low” rate the uncertainties of the resonance parameters were inserted. For the calculation of the “high” reaction rate we used the full upper limit for the hypothetical resonance at 635 keV in addition to the other resonances. The results are given in Table II. It is obvious that there are substantial differences from the rates given in [11] and [12], especially with respect to the uncertainties. Käppeler *et al.* [12] assumed higher $\omega\gamma$ values for the resonances at 635 and 832 keV, while NACRE [11] chose a constant S factor as the assumed contribution of possible resonances in the energy range from threshold up to about 820 keV. For the NACRE high rate, all known states in ^{26}Mg [19,20] were considered, as also done by

TABLE III. Parameters a_i , b_i , and c_i (with significant digits) for the same analytical expression of the reaction rate of $^{22}\text{Ne}(\alpha, n)^{25}\text{Mg}$ as employed in the NACRE compilation [11], given for the recommended function (left), and the band of uncertainty with a high rate (upper right) and a low rate (lower right).

i	a_i		b_i		c_i	
1	4.04	3.68 4.55	0	0 0	7.74	7.70 7.781
2	2.302×10^{-4}	9.02×10^{-4} 1.701×10^{-10}	-0.60	-1.70 -5.98	6.14	6.31 6.22
3	6900	10 900 8000	3.19	2.853 2.75	11.3	11.6 11.55
4	1.881×10^7	5.21×10^6 1.003×10^6	0.358	1.05 1.50	26.7	23.2 23.0

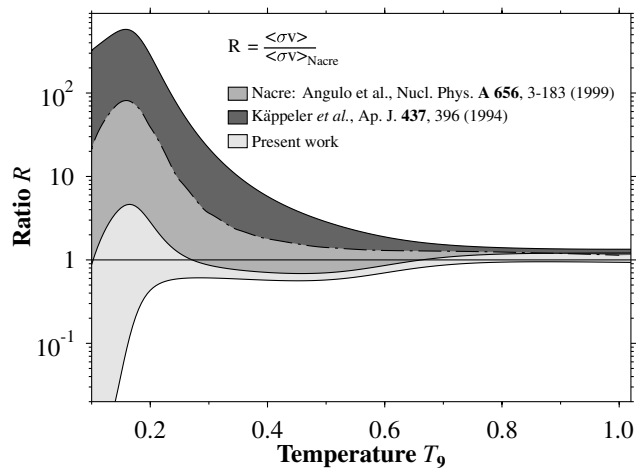


FIG. 2. Comparison of the bands of uncertainty, marked with different grey scales, obtained for the reaction rate of $^{22}\text{Ne}(\alpha, n)^{25}\text{Mg}$ from the determination of this work and the compilations of Käppeler *et al.* [12] and NACRE [11]. All rates have been normalized here to NACRE. At $T_9 = 0.2$ the reduction of the uncertainty obtained in the present work is about a factor of 100.

Drotleff *et al.* [8] as an extreme assumption. The two assumptions are responsible for the higher NACRE rate for $T_9 < 0.2$ [$T_9 = T/(10^9 \text{ K})$].

We have calculated an analytical expression for the reaction rates, employing the same parametrization as NACRE. This expression is valid in the full temperature range of $0.1 \leq T_9 \leq 10$, and reproduces the tabular values within an accuracy of about 8%. The parameters a_i , b_i , and c_i of this expression are given in Table III for the recommended, high, and low rates,

$$N_A \langle \sigma v \rangle = \sum_{i=1}^4 a_i T_9^{b_i} \exp(-c_i/T_9).$$

For $T_9 > 0.6$ all four reaction rates in Table II are in fair agreement in both magnitude and temperature dependence. For $0.1 \leq T_9 \leq 0.6$ the differences between the data sets noticeably increase as far as the absolute values, the temperature dependences, and the bands of uncertainty are concerned. At $T_9 = 0.2$ the uncertainty given by NACRE [11] was a factor of ~ 500 (high:adopted). In the present work this uncertainty was reduced to a factor of 5, as shown in Fig. 2. In the compilation of Käppeler *et al.* [12] this ratio was only 2, but at a much higher absolute level of the reaction rate (see Table II), the rate of Käppeler *et al.* being a factor of 28 higher than the present value. On the other hand, the NACRE rate is $\sim 40\%$ higher than the present one, which is within the limits of error. At still lower temperatures the differences and uncertainties get larger, but one has to keep in mind that for $T_9 \leq 0.18$ the competing (α, γ) reaction becomes dominant [12].

Because of the interplay of many reactions, the influence on nucleosynthesis of a change in one specific reaction rate can be very complex, and can be studied properly only within the framework of a complete stellar reaction network.

In conclusion, the present work significantly improves our knowledge of the reaction rates at all temperatures. In particular, for $T_9 > 0.2$, where the $^{22}\text{Ne}(\alpha, n)^{25}\text{Mg}$ neutron production will be large enough to be effective in the *s* process, the improved rates justify new computations of the *s* process in massive stars. The new rates completely rule out the large enhancements of the $^{22}\text{Ne}(\alpha, n)^{25}\text{Mg}$ rate suggested by some recent *s* process calculations [14,16]. Preliminary calculations with our new reaction rates reproduce the *s* process abundances much better than the older, higher rates [21].

We are indebted to U. Kneissl for supporting this project. We thank S. E. Woosley, A. Heger, and P. Mohr for reading the manuscript and for their valuable comments. This work was supported by the Deutsche Forschungsgemeinschaft.

-
- [1] F. Käppeler *et al.*, Rep. Progr. Phys. **52**, 945 (1989).
 - [2] S. E. Woosley and T. A. Weaver, Astrophys. J. Suppl. Ser. **101**, 181 (1995).
 - [3] R. Gallino *et al.*, Astrophys. J. **333**, L25 (1988).
 - [4] F. X. Haas and J. K. Bair, Phys. Rev. C **7**, 2432 (1973).
 - [5] K. Wolke *et al.*, Z. Phys. A **334**, 491 (1989).
 - [6] V. Harms *et al.*, Phys. Rev. C **43**, 2849 (1991).
 - [7] H. W. Drotleff *et al.*, Z. Phys. A **338**, 367 (1991).
 - [8] H. W. Drotleff *et al.*, Astrophys. J. **414**, 735 (1993).
 - [9] U. Giesen *et al.*, Nucl. Phys. **A561**, 95 (1993).
 - [10] R. Kunz *et al.*, in *Proceedings of the 4th International Conference on Applications of Nuclear Techniques "Neutrons and their Applications," Crete, Greece, 1994*, edited by G. Vourvopoulos and Th. Paradellis, SPIE Proceedings Vol. 2339 (SPIE-International Society for Optical Engineering, Bellingham, WA, 1995), pp. 38-55.
 - [11] C. Angulo *et al.*, Nucl. Phys. **A656**, 3 (1999).
 - [12] F. Käppeler *et al.*, Astrophys. J. **437**, 396 (1994).
 - [13] G. R. Caughlan and W. A. Fowler, At. Data Nucl. Data Tables **40**, 283 (1988).
 - [14] V. Costa *et al.*, Astron. Astrophys. **358**, L67 (2000).
 - [15] G. Wallerstein *et al.*, Rev. Mod. Phys. **69**, 995 (1997).
 - [16] L.-S. The *et al.*, Astrophys. J. **533**, 998 (2000).
 - [17] J. W. Hammer, in *Proceedings of the International Workshop XXVI on Gross Properties of Nuclei and Nuclear Excitations, Hirschegg, Austria*, edited by M. Buballa, W. Nörenberg, J. Wambach, and A. Wirzba (GSI, Darmstadt, 1998), ISSN 0720-8715, p. 370.
 - [18] P. M. Endt, Nucl. Phys. **A633**, 1 (1998).
 - [19] B. L. Berman *et al.*, Phys. Rev. Lett. **23**, 386 (1969).
 - [20] H. Weigmann *et al.*, Phys. Rev. C **14**, 1328 (1976).
 - [21] A. Heger and S. E. Woosley (private communication).